**Paper:**
Zeis, T., Howell, O., Reynolds, R. & Schaeren-Wiemers, N. (2018). Molecular pathology of Multiple Sclerosis lesions reveals a heterogeneous expression pattern of genes involved in oligodendrogliogenesis. *Experimental Neurology*
http://dx.doi.org/10.1016/j.expneurol.2018.03.012

Experimental Neurology 305 (2018) 76–88

Contents lists available at ScienceDirect

Experimental Neurology

journal homepage: www.elsevier.com/locate/yexnr

Research Paper

# Molecular pathology of Multiple Sclerosis lesions reveals a heterogeneous expression pattern of genes involved in oligodendrogliogenesis

T. Zeis[a], O.W. Howell[b], R. Reynolds[c], N. Schaeren-Wiemers[a,*]

[a] Neurobiology, Department of Biomedicine, University Hospital Basel, University Basel, Zentrum für Lehre und Forschung, Basel, Switzerland
[b] Institute of Life Sciences, Swansea University Medical School, Swansea SA2 8PP, UK
[c] Division of Brain Sciences, Faculty of Medicine, Imperial College London, Hammersmith Hospital Campus, London W12 0NN, UK

ARTICLE INFO

*Keywords:*
Multiple Sclerosis
Gene expression analysis
Molecular pathology
Oligodendrogliogenesis
STAT6 pathway
Multiple Sclerosis lesions

ABSTRACT

Little is known about the decisive molecular factors that regulate lesion remyelination in Multiple Sclerosis. To identify such factors, we performed a differential gene expression analysis of normal appearing white matter (NAWM), active, remyelinating, and inactive demyelinated lesions. As expected, many genes involved in inflammatory processes were detected to be differentially regulated between these tissue types. Among them, we found an increased expression of members of the STAT6 pathway such as STAT6, IL4 and IL4R in active, remyelinated and inactive demyelinated lesions. This suggests that a protective, anti-inflammatory reaction, as already reported to be present in MS NAWM, is further enhanced in lesion tissues. Focusing on genes influencing oligodendrogliogenesis, we found a decreased expression of NKX2-2 in active, remyelinated and inactive demyelinated lesions, whereas SOX10 was downregulated in inactive demyelinated lesions, when compared to NAWM. Simultaneously, CXCL12 (SDF1) expression was strongly increased in active, remyelinated and inactive demyelinated lesions, but increased expression of the IGF1 and IGF2 genes was found in inactive demyelinated lesions. This demonstrates that, in principle, expression of genes promoting oligodendrogliogenesis occurs in MS lesion tissue - even in inactive demyelinated lesions. In contrast, oligodendrogenesis inhibiting genes such as JAG1 were also expressed at higher levels in inactive demyelinated lesions. Both, oligodendrogliogenesis promoting as well as inhibiting genes are expressed in all lesion tissues. However, no clear promoting or inhibiting expression pattern could be detected in any of the different types of lesioned tissues. This might reflect the heterogeneity of lesion development in MS patients, both in terms of mechanisms and temporal differences.

## 1. Introduction

Multiple Sclerosis (MS) is a chronic inflammatory, demyelinating disease of the central nervous system (CNS) with a large degree of heterogeneity in clinical course and histopathology (Compston and Coles, 2002). It is suggested that MS is an autoimmune disorder directed against CNS antigens, which leads to inflammation and demyelination (Hemmer et al., 2002; Noseworthy et al., 2000). However, other findings suggest that the primary cause for inflammation in MS could be primary oligodendrocyte degeneration (Barnett and Prineas, 2004; Trapp, 2004). One major characteristic of MS is the formation of the so-called plaques or lesions; areas of demyelination in the white matter with variable levels of axonal damage (Lassmann, 1998) (Fig. 1). The mechanisms underlying early lesion development are still unclear, but are thought to involve altered BBB permeability and nodules of activated microglial (van der Valk and Amor, 2009) in the normal appearing tissue, in which sub-pathological changes have been shown to be present (Filippi et al., 1998; Graumann et al., 2003; Lindberg et al., 2004; Zeis et al., 2008). Some of these areas of microglial activation are suggested to transform into full, active demyelinating lesions characterized by massive infiltration of immune cells, primarily of the monocyte/macrophage lineage.

There is evidence that remyelination in the MS brain can be extensive, although highly heterogeneous (Trapp, 2004), and may be initiated in rapid succession following demyelination (Prineas et al., 1989; Raine and Wu, 1993). Depending on whether the process of repair and remyelination prevails over demyelination or not, active lesions develop into inactive demyelinated lesions, partially remyelinated or fully remyelinated lesions. To remyelinate, oligodendrocyte progenitor cells (OPCs) are recruited to repopulate the area of demyelination, differentiate into oligodendrocytes and remyelinate the demyelinated axons (Franklin, 2002). During these steps, OPCs have to

*Abbreviations:* AL, active lesion; RL, remyelinating lesion; IdL, Inactive demyelinating lesion; NAWM, normal appearing white matter

* Corresponding author at: Neurobiology, Department of Biomedicine, University Hospital Basel, University Basel, Hebelstrasse 20, CH-4031 Basel, Switzerland.
*E-mail address:* Nicole.schaeren-wiemers@unibas.ch (N. Schaeren-Wiemers).

https://doi.org/10.1016/j.expneurol.2018.03.012
Received 11 November 2017; Received in revised form 28 February 2018; Accepted 16 March 2018
Available online 27 March 2018

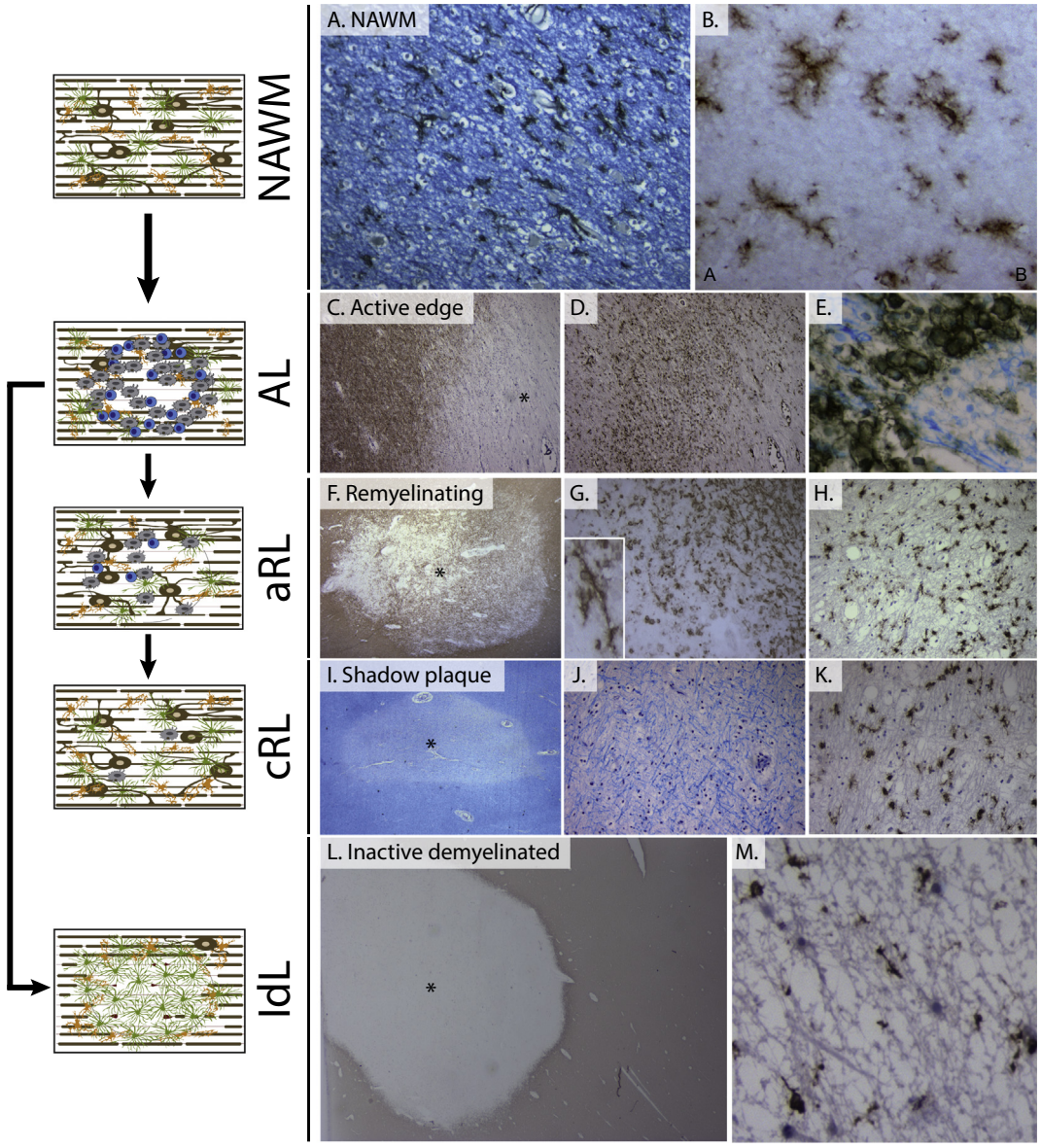


**Fig. 1.** Tissue characterization.
All tissue blocks were stained with LFB (A, E, I, J), anti-HLA-DR (LN3, A, B, D, E, H, K, M) and anti-MOG (C, L) antibodies. Accordingly, tissue was characterized and subsequent sections selected for the micro-dissection of tissue for total RNA isolation. Normal appearing white matter tissue showed normal, non-pathological myelin (A) and microglia with a surveilant and ramified morphology (A, B). In contrast, active lesions showed a loss of myelin (C) as well as activated microglia/macrophages containing myelin lipids (D, E). Remyelinating tissue was either characterized as partially remyelinated lesions containing MOG + oligodendrocytes and short myelin internodes in areas of ongoing inflammation (F, G and H) termed as active RL (aRL) or completely remyelinated (cRL) and characterized by the pale myelin staining (LFB) of the shadow plaque (I, J) accompanied by modest numbers of activated microglia/macrophages (K). Inactive demyelinated tissue showed a complete demyelination (L) without significant active inflammation or myelin debris (M). Left panels: Schematic drawing of MS lesions show the simplified cellular situation in the specified tissue in order to visualize the cellularity defining the mRNA isolated. Oligodendrocytes and their myelin sheets (brown), astrocytes (green), microglia (yellow) as well as activated microglia/macrophage (grey) and other infiltrating immune cells of various types (blue) are shown. Asterisks = lesion tissue. (For interpretation of the references to color in this figure legend, the reader is referred to the web version of this article.)

migrate, proliferate and differentiate; processes that have to be tightly controlled by numerous molecular events, including axonal electrical activity (Franklin, 2002; Franklin and Ffrench-Constant, 2008; Gautier et al., 2015). Failure of remyelination results in inactive demyelinated lesions, in which myelin has been removed, immune cells are largely absent and the remaining demyelinated axons are embedded in a glial scar (Compston et al., 2006).

Substantial progress has been made in understanding the molecular mechanisms of remyelination. However, the overall nature and timing of molecular signaling influencing remyelination in MS lesion development and resolution are still incompletely understood. To identify genes involved in lesion formation and resolution, we performed a differential gene expression analysis between the distinct histological tissue types from brain autopsies of MS cases: normal appearing white matter (NAWM), active lesions (AL), remyelinating lesions (RL) and inactive demyelinated lesions (IdL). We found several genes involved in inflammatory processes to be differentially regulated. We further aimed to identify genes known to be involved in oligodendrogliogenesis in order to identify potential key factors in oligodendrocyte repair/remyelination. In all tissues, we found altered expression of genes both promoting and inhibiting oligodendrogliogenesis. Our study shows that the molecular pattern of pathohistologically similar tissues can be quite

**Table 1**
Patient characterization.
Summary of clinical data and characterization of MS cases. Clinical and pathological information concerning the 7 progressive MS cases studied are shown. NAWM, normal appearing white matter, AL, active lesion, RL, remyelinating lesion, IdL, inactive demyelinated lesion.

| Patient ID | Age (yr) | Sex | MS type | Disease duration (yrs) | Postmortem interval (hrs) | Cause of death | NAWM | AL | RL | IdL |
|---|---|---|---|---|---|---|---|---|---|---|
| MS40 | 48 | F | PP | 21 | 6 | Bronchopneumonia | 2 | 1 | 1 | 1 |
| MS79 | 49 | F | SP | 23 | 7 | Bronchopneumonia | 1 | 1 | 1 | 1 |
| MS106 | 39 | F | PP | 21 | 18 | Bronchopneumonia | 1 | 2 | 1 | 1 |
| MS122 | 44 | M | SP | 16 | 16 | Bronchopneumonia | 1 | 3 | 2 | 1 |
| MS136 | 40 | M | SP | 9 | 10 | Respiratory failure, sepsis | 2 | 1 | 1 | 1 |
| MS154 | 34 | F | SP | 11 | 12 | Pneumonia | 1 | 1 | – | – |
| MS176 | 37 | M | PP | 27 | 12 | Intestinal obstruction | 1 | – | 1 | – |

**Table 2**
Antibodies.
Antibodies used in this study. Table shows all antibodies, their origin and dilution used. Abbreviations: dk-a-rb, donkey anti rabbit; dk-a-m, donkey anti mouse; dk-a-gt, donkey anti goat.

| Antibody | Company | Cat.Nr. | Dilution |
|---|---|---|---|
| Primary antibodies | | | |
| anti-MOG (Clone Z12) | Kindly provided by Prof. R.Reynolds | – | 1:200 |
| anti-NEUN | Millipore | MAB377 | 1:500 |
| anti-GFAP | Sigma-Aldrich | G-3893 | 1:2000 |
| anti-CD68 | Abcam | ab845 | 1:500 |
| anti-LN3 | Abcam | ab49388 | 1:500 |
| anti-OLIG2 | Millipore | ab9610 | 1:500 |
| Secondary antibodies | | | |
| dk-a-rb-Biotin | Jackson ImmunoResearch | 711-065-152 | 1:500 |
| dk-a-m-Biotin | Jackson ImmunoResearch | 715-065-151 | 1:500 |
| dk-a-gt-Biotin | Jackson ImmunoResearch | 705-065-147 | 1:500 |

variable, possibly reflecting the heterogeneity of lesion development and repair in MS brain tissue.

## 2. Materials and methods

### 2.1. Tissue collection

MS and control tissue samples were supplied by the UK Multiple Sclerosis Tissue Bank (UK Multicentre Research Ethics Committee, MREC/02/2/39), funded by the Multiple Sclerosis Society of Great Britain and Northern Ireland (registered charity 207,495). For this study, tissue samples representing different tissue types were isolated from a total of 7 progressive MS cases (4 SPMS, 3 PPMS; Table 1). The median disease duration was 21 years (range from 11 to 27). The median age at death was 40 years (range from 34 to 49). Altogether, 7 remyelinating lesions, 9 NAWM regions, 9 active lesions and 5 inactive demyelinated lesions were dissected (see Table 1). All brains had been screened by a neuropathologist to confirm diagnosis of MS and to exclude other confounding pathologies. All tissues were screened for the presence of T-cells (CD3), activated microglia and macrophages (CD68), activated astrocytes (GFAP) and signs of demyelination and remyelination (MOG, PLP) (Fig. 1). Regions of interest for RNA isolation were dissected manually from several 20 µm cryosections per block. In regular intervals, sections were analysed by immunohistochemistry to confirm tissue characteristics and to exclude contamination of the dissected tissue sample with other tissue types.

### 2.2. Tissue characterization and definition

Immunostaining against MOG and HLA-DR, as well as Luxol fast blue (LFB) histology, were performed to characterize and differentiate the tissue types (Fig. 1), as suggested by Kuhlmann et al. (Kuhlmann et al., 2017). NAWM tissue was characterized by a normal myelin (Fig. 1A) and microglial staining at least 10 mm from areas of visible demyelination (Fig. 1A, B). Active lesions (AL) showed a loss of myelin (Fig. 1C) and the presence of activated microglia/macrophages containing myelin debris (Fig. 1D, E). Remyelinating tissue was characterized by pale or thinly myelinated fibres with MOG+ oligodendrocytes in areas of ongoing inflammation (Fig. 1F, G and H) or characterized by areas of pale LFB+ myelin staining (Fig. 1I, J) with some residual activated microglia/macrophages (Fig. 1K). Inactive demyelinated lesions (IdL) were completely demyelinated with a well demarcated border (Fig. 1L) and very few macrophages (Fig. 1M).

### 2.3. Immunohistochemistry

All tissue samples were analysed by immunohistochemistry. Cryostat sections (10 µm) used for tissue characterization using anti-HLA-DR, -MBP and -MOG antibodies were fixed for 10 min in 10% formalin. For inactivation of endogenous peroxidase, all sections were treated with 0.3% hydrogen peroxide and blocked with blocking buffer (1% normal donkey serum, 2% Fish skin gelatin, 0.15% Triton). After quenching, sections were incubated with primary antibodies overnight at 4 °C. Secondary biotinylated antibodies were applied for 1 h at room temperature followed by the ABC complex reagent (Vector Labs) for 1 h. Color reaction was performed with 3-amino-9-ethylcarbazole or diaminobenzidine (Erne et al., 2002). Counterstaining was performed in haematoxylin for 1 min followed by rinsing the slide in running tap water. Antibodies used are shown in Table 2.

### 2.4. Total RNA preparation

Serial sections (20 µm) were prepared, following tissue characterization and identification of regions of interest (above), for the isolation of total RNA. Tissue was isolated by micro-dissecting areas of NAWM, AL, aRL, cRL or Idl with reference to the characterized sections from a minimum of 3 serial 20 µm sections. At regular intervals, sections were analysed by immunohistochemistry to confirm tissue characteristics and to exclude contamination of tissue sample with other tissue types. Samples were handled and cut in such a way that they never thawed and the cryostat, dissecting equipment and collection tubes were treated with RNaseZap (ThermoFisher Scientific) or certified free of RNase/DNase contamination. Total RNA isolation was performed by homogenizing the tissue in guanidinium thiocyanate followed by a CsCl ultracentrifugation (Graumann et al., 2003). Freshly isolated RNA was tested for integrity using an Agilent 2100 Bioanalyser instrument (Agilent, Santa Clara, California, USA; all samples had an RNA Integrity Number of > 7) and by Northern blot analysis for the expression of GFAP mRNA, as previously described (Graumann et al., 2003).

### 2.5. Atlas™ cDNA expression array hybridization

For this analysis, a custom made Clontech Atlas™ cDNA Expression Array was made which contains 1′185 selected cDNA sequences on a nylon membrane. Genes spotted on the nylon membrane were based on

the data of earlier gene expression studies (Graumann et al., 2003 and Zeis et al., 2008) as well as on literature searches for genes involved in oligodendrogenesis (detailed list is found in Supporting information Table S1) resulting in an array focused on CNS and especially oligodendrogliogenesis relevant genes. Array hybridization was performed according to Graumann et al., (2003). Hybridization signals were detected with the phosphoimaging system (GE Healthcare Europe, Amersham, Molecular Dynamics, Glattbrugg, Switzerland). Differential gene expression analysis was made with 30 total RNA samples of different origin from 7 patients (Table 1). From 1′185 genes present on the array, 1099 genes were detectable at least in one tissue group (NAWM, AL, RL and IdL), whereas 86 were not detectable in any tissue groups.

### 2.6. qRT-PCR

Quantitative RT-PCR was performed in 384-well plates (VWR, Radnor, USA, Cat.No. 82006-678) using the ABI ViiA Fast Real-Time PCR system (Applied Biosystems, Life technologies Ltd., Paisley, UK). Primer sequences were designed from unique sites over exon–intron junctions to prevent amplification of genomic DNA. Real-time RT-PCR was performed according to the manufacturer's protocol using the KAPA SYBR Fast Universal 2× qPCR Master mix (KAPA Biosystems, Woburn, USA). RNA amounts were calculated with relative standard curves for all mRNAs of interest. qRT-PCR was normalized with the H1FX, RPL3 and RPS6KA3 housekeeping genes.

### 2.7. Gene expression analysis, statistics and pathway analysis

Quantification of differential hybridization signal intensities was achieved with the AtlasImage™ 2.0 software program. A log2 transformation was then applied to the raw intensity values of each array. Normalization was completed using the quantile normalization method. Expression data were analysed using R and the software package limma (Phipson et al., 2016; R developmental Core Team, 2008; Ritchie et al., 2015). Statistical analysis was performed using the linear model with tissue type, patient and batch as factors. Genes with a p-value below 0.05 ($p < 0.05$) were considered significantly changed between groups. Fold changes above 1.5 are considered to be higher expressed, whereas fold changes below −1.5 are considered to be lower expressed in the different tissue types. Data were further analysed with IPA (Ingenuity® Systems, www.ingenuity.com). All genes with a fold change higher/lower than ± 1.5 were used for the ingenuity pathway analysis. Analysis was performed comparing all different tissue types.

## 3. Results

### 3.1. Similarities and differences in gene expression between the different MS tissue types

As a first step, we performed LFB staining as well as a detailed immunohistochemical analysis of all MS brain tissues to identify the different tissue types (NAWM, AL, RL and IdL; Fig. 1), a prerequisite for our differential gene expression analysis. All gene expression data were compared between the different tissue types (Fig. 2, Supporting information Table S1), representative for specific stages in lesion development (Fig. 1).

To identify genes which might be involved in the initiation further development of lesions, we first compared the gene expression patterns between AL and NAWM. From the 1185 genes present on the array, 47 were significantly differentially expressed ($p < 0.05$, $|FC| > 1.5$) between AL and NAWM (Fig. 2A). Among them, 17 had increased and 30 decreased expression in AL tissue.

A comparison between RL tissue, which is in the process or at the end of remyelination, and NAWM would be expected to reveal genes involved in remyelination or genes involved in the maintenance of oligodendrocytes. This comparison between RL and NAWM revealed 57 genes to be significantly differentially expressed. Expression of 28 genes was increased, whereas the expression of 29 genes was reduced in RL tissue (Fig. 2B).

Comparing gene expression of NAWM with IdL would be expected to reveal significant reduction in expression of oligodendrocyte specific genes due to the oligodendrocyte loss in IdL. Furthermore, this comparison serves as a positive experimental control, as myelin gene expression was reduced as anticipated in IdL lesions compared to NAWM (Fig. 2C). Finally, genes involved in the initiation or regulation of oligodendrogliogenesis might either be up- or downregulated in IdL. Reflecting the cellular changes, the most significantly differentially expressed genes were found between IdL and NAWM, where 50 genes were increased and 110 genes were decreased in IdL (Fig. 2C).

The comparison of AL and RL potentially reveals genes that are necessary for the initiation of remyelination. However, the fewest significantly differentially expressed genes were found between AL and RL. Only 3 genes were significantly increased and 6 genes significantly decreased in AL tissue in comparison to RL (Fig. 2D). Differences in gene expression between AL and IdL might be expected to reveal genes inhibiting remyelination and/or promoting astrogliogenesis/scar formation. Comparison between AL and IdL revealed 74 significantly differentially expressed genes, of which 55 were increased and 19 decreased, in AL tissue (Fig. 2E). Comparing RL and IdL gene expression should reveal genes involved in remyelination or genes inhibiting remyelination. 33 genes were found to be significantly differentially expressed between RL and IdL tissues. Expression of 23 genes was increased and 10 decreased in RL tissue (Fig. 2F).

A summary of the top 30 most changed genes between all tissue types and possibly the most relevant in lesion development and resolution is shown in Table 3. A detailed list of all differentially expressed genes can be found in Supporting information Table S1.

### 3.2. Comparison of remyelinating and chronic silent lesions did not reveal a clear promotion of oligodendrogliogenesis

In RL tissue, remyelination has either already taken place or is ongoing. In contrast, in IdL it is assumed that remyelination has failed. Therefore, it might be expected that this comparison might reveal genes important for remyelination or inhibition thereof. Analysis of differential gene expression of RL vs IdL, however, did not reveal a clear result. As expected, we detected a reduced expression of several genes known to be expressed in oligodendrocytes in IdL, such as e.g. GJB1, MAG, SOX10 or MAL (Table 4). We then searched for genes influencing oligodendrogliogenesis in RL and found JAG2 expression, known to inhibit oligodendrogliogenesis, to be reduced in RL vs IdL ($p = 0.02$, Table 4). We also found CNTN2 ($p = 0.01$) and SOX10 (0.01), both known to promote oligodendrogliogenesis (Zoupi et al., 2018), to be more highly expressed in RL. In contrast, expression of IGF2 ($p = 0.01$) and MARCKS ($p = 0.05$), both thought to positively influence oligodendrogliogenesis, were reduced in RL than in IdL (Table 4). Altogether, no clear pattern of genes promoting or inhibiting oligodendrogliogenesis was detected between RL and IdL tissue.

### 3.3. Cluster analysis reveals heterogeneity between the different tissue types

To analyze and characterize the differential gene expression between NAWM, AL, RL and IdL in more detail, a cluster analysis was performed (Fig. 3). Basically, three clusters were detected. Cluster I mainly included NAWM (Fig. 3). Six out of 9 NAWM samples were found in cluster I whereas one was found in cluster II and two in cluster III. Cluster II included most IdL tissue samples of which 4 of 5 were found in this cluster (Fig. 3). One IdL sample was found in cluster III. Both AL and RL tissue samples were dispersed throughout all three clusters and did not separate in two separate clusters, despite some similarities in immunohistological appearance. No clustering was detected when the confounding factors, batch and patient, were analysed.

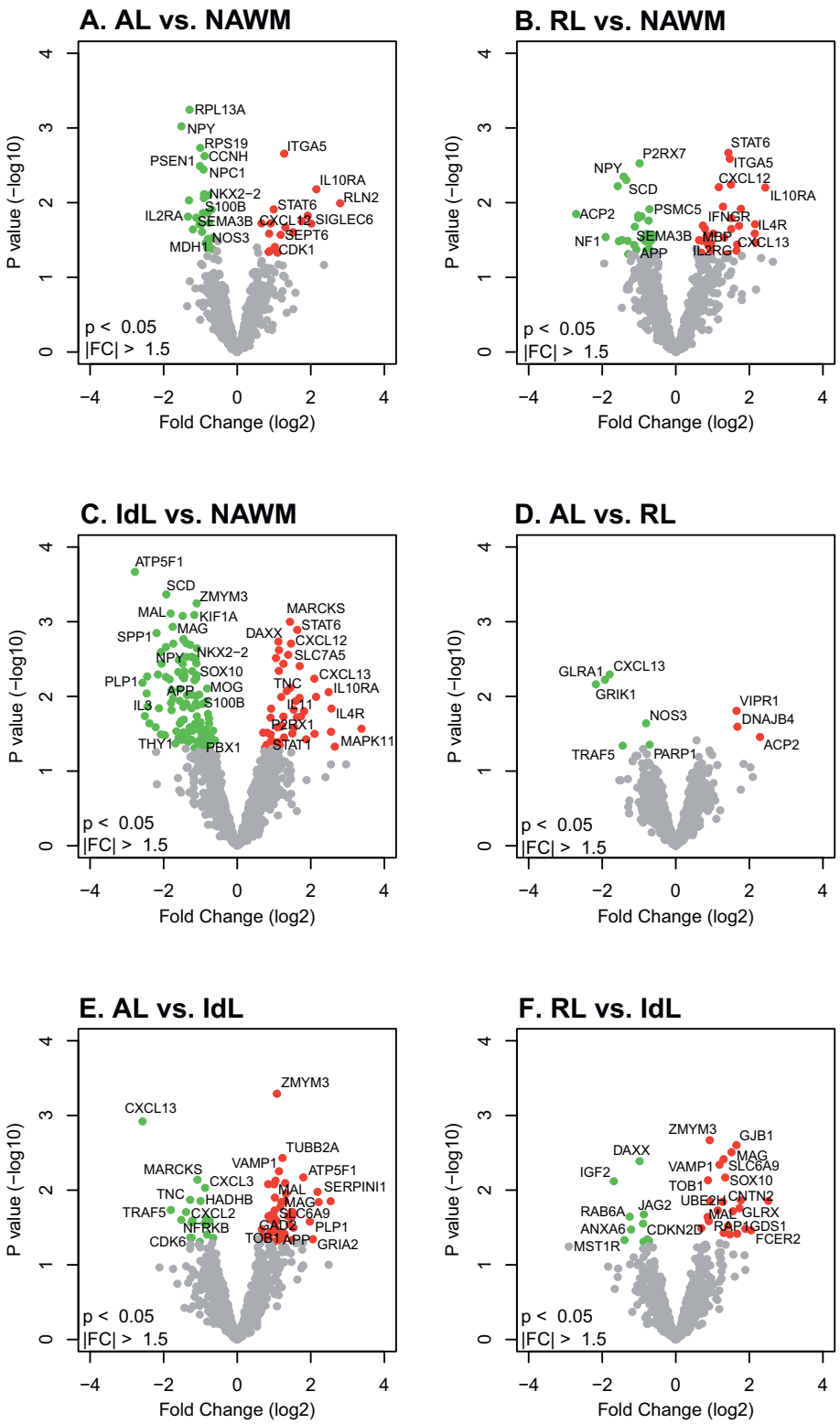


**Fig. 2.** Differential gene expression between the different tissues.
Volcano plots of the differential gene expression in between the different tissues. All possible comparisons are shown. However, for better visibility, only a selection of gene names is shown. All genes with a p-value of $< 0.05$ and a fold change of $+/-$ 1.5 are marked by red or green color, respectively. Most significantly differential expressed genes were found between NAWM and IdL whereas the AL and RL tissues seemed to be the most similar. (For interpretation of the references to color in this figure legend, the reader is referred to the web version of this article.)

**Table 3**
Top genes showing most significant changes between the different MS tissue types.

30 genes with most significant changes in gene expression between the different tissue types is shown. Genes with a p-value of < 0.05 are marked by a grey background color and were further colored according to their fold change. Genes with a fold change higher than 1.5 were marked red. Genes with a fold change lower than −1.5 were marked green.

| | | AL | | | RL | | IdL |
|---|---|---|---|---|---|---|---|
| | | NAWM | RL | IdL | NAWM | IdL | NAWM |
| SYMBOL | Gen name | FC | FC | FC | FC | FC | FC |
| CXCL13 | chemokine (C-X-C motif) ligand 13 (B-cell chemoattractant) | -1.39 | -3.47 | -5.95 | 2.50 | -1.71 | 4.28 |
| PARP1 | ADP-ribosyltransferase (NAD+; poly (ADP-ribose) polymerase) | -1.01 | -1.64 | -1.78 | 1.62 | -1.09 | 1.77 |
| PEA15 | astrocytic phosphoprotein PEA-15 | -1.03 | 1.48 | 1.48 | -1.52 | -1.00 | -1.52 |
| SCD | ACYL-COA DESATURASE (EC 1.14.99.5) (STEAROYL-COA DESATURASE) (FATTY ACID DESATURASE) (DELTA(9)-DESATURASE). | -1.81 | 1.40 | 2.10 | -2.54 | 1.50 | -3.80 |
| ACVRL1 | activin A receptor type II-like 1 | 4.04 | -1.10 | -1.06 | 4.46 | 1.04 | 4.30 |
| ALCAM | CD166 ANTIGEN PRECURSOR (ACTIVATED LEUKOCYTE-CELL ADHESION MOLECULE) (ALCAM). | -1.51 | 1.13 | 2.78 | -1.70 | 2.47 | -4.20 |
| APP | Alzheimer's disease amyloid A4 protein precursor; protease nexin-II (PN-II); APPI | -1.33 | 1.58 | 2.23 | -2.10 | 1.41 | -2.95 |
| ATP5F1 | ATP SYNTHASE B CHAIN, MITOCHONDRIAL PRECURSOR | -1.98 | 1.19 | 3.48 | -2.35 | 2.93 | -6.88 |
| CHRNA6 | cholinergic receptor, nicotinic, alpha polypeptide 6 | -2.30 | -2.26 | 1.51 | -1.02 | 3.41 | -3.48 |
| COX5B | CYTOCHROME C OXIDASE POLYPEPTIDE VB PRECURSOR (EC 1.9.3.1). | -1.62 | 1.03 | 1.07 | -1.67 | 1.04 | -1.74 |
| CXCL12 | chemokine (C-X-C motif) ligand 12 (stromal cell-derived factor 1) | 1.88 | -1.20 | -1.47 | 2.25 | -1.22 | 2.76 |
| DAXX | death-associated protein 6 | 1.38 | 1.26 | -1.57 | 1.10 | -1.98 | 2.17 |
| DYNLL1 | cytoplasmic dynein light chain 1 (HDLC1); protein inhibitor of neuronal nitric oxide synthase (PIN) | -1.88 | 1.02 | 1.49 | -1.91 | 1.46 | -2.79 |
| EDIL3 | INTEGRIN BINDING PROTEIN DEL-1. | -1.54 | 1.04 | 2.89 | -1.61 | 2.77 | -4.45 |
| ELAVL3 | HU-ANTIGEN C (PARANEOPLASTIC CEREBELLAR DEGENERATION-ASSOCIATED ANTIGEN). | -1.18 | 1.13 | 2.06 | -1.33 | 1.82 | -2.43 |
| FSCN1 | FASCIN (ACTIN BUNDLING PROTEIN). | -1.14 | 1.52 | 2.00 | -1.73 | 1.32 | -2.28 |
| GJB1 | GAP JUNCTION BETA-1 PROTEIN (CONNEXIN 32) (CX32) (LIVER GAP JUNCTION PROTEIN) | -1.33 | -1.25 | 2.51 | -1.06 | 3.14 | -3.34 |
| GSTO1 | glutathione-S-transferase like; glutathione transferase omega | -1.90 | 1.07 | 1.02 | -2.03 | -1.04 | -1.95 |
| IL10RA | interleukin 10 receptor, alpha | 4.45 | -1.21 | -1.26 | 5.40 | -1.04 | 5.60 |
| IL2RA | interleukin 2 receptor, alpha | -2.53 | -1.02 | 1.00 | -2.48 | 1.02 | -2.53 |
| ITGA5 | integrin, alpha 5 (fibronectin receptor, alpha polypeptide) | 2.42 | -1.14 | -1.05 | 2.77 | 1.09 | 2.54 |
| ITSN1 | intersectin 1 (SH3 domain protein) | 1.58 | -1.05 | -1.31 | 1.67 | -1.25 | 2.08 |
| JAG2 | jagged 2 | 1.07 | 1.04 | -1.76 | 1.03 | -1.82 | 1.88 |
| KCNJ2 | cardiac inward rectifying potassium channel 2 (KCNJ2); HIRK1; KIR2.1 | -1.72 | -1.07 | 1.27 | -1.61 | 1.36 | -2.19 |
| KIF1A | kinesin-like protein KIF1A; axonal transporter of synaptic vesicles | -1.25 | 1.24 | 1.79 | -1.56 | 1.44 | -2.25 |
| MAG | myelin-associated glycoprotein precursor (MAG) | -1.46 | -1.24 | 2.30 | -1.18 | 2.86 | -3.37 |
| MAL | mal, T-cell differentiation protein | -1.42 | 1.12 | 2.47 | -1.59 | 2.20 | -3.50 |
| MARCKS | myristoylated alanine-rich C-kinase substrate (MARCKS); protein kinase C substrate 80-kDa protein light chain (PKCSL) | 1.28 | -1.24 | -2.11 | 1.58 | -1.71 | 2.70 |
| MOG | myelin-oligodendrocyte glycoprotein precursor (MOG) | -1.44 | 1.01 | 1.23 | -1.46 | 1.21 | -1.76 |
| NPY | neuropeptide Y | -2.86 | -1.07 | 1.05 | -2.67 | 1.13 | -3.00 |
| PIP4K2A | phosphatidylinositol-4-phosphate 5-kinase type III (PIP5K3); PTDINS(4)P-5-kinase C isoform; diphosphoinositide kinase + phosphatidylinositol-4-phosphate 5-kinase type II alpha (PIP5K2A); PTDINS(4)P-5-kinase B isoform | -1.45 | 1.07 | 2.87 | -1.56 | 2.68 | -4.16 |

### *3.4. Genes involved in oligodendrogliogenesis are differentially expressed between NAWM, AL, RL and IdL*

For successful remyelination to occur, OPCs have to become activated, recruited to the lesion area and differentiate into remyelinating oligodendrocytes (Franklin and Ffrench-Constant, 2008). By analyzing the differential gene expression pattern, we found altered expression of many genes influencing oligodendrogliogenesis (Table 4, Fig. 5) in a positive and negative way in all the different tissue types.

We found the expression of IGF1, reported to influence oligodendrogliogenesis (Beck et al., 1995; Carson et al., 1993; Huang and Dreyfus, 2016; McMorris et al., 1986), to be significantly elevated in IdL in comparison to NAWM ($p = 0.019$, Fig. 4A). In comparison to NAWM, IGF1 expression was increased in some AL and RL, but this was not a consistent result. IGF1 and IGF2 expression were significantly increased in IdL in comparison to NAWM ($p = 0.015$). IGF2 expression was significantly reduced in RL in comparison to IdL ($p = 0.008$, Fig. 4B). Fibroblast growth factors, such as FGF2 and FGF9, have been reported to be involved in oligodendrocyte maturation (Fortin et al., 2005; Furusho et al., 2012; Lindner et al., 2015; McKinnon et al., 1990). However, we found no significant difference in FGF expression between the analysed tissue types. Some cases showed a strong increase in FGF2

and FGF9, whereas in others FGFs were down regulated. FGFR4 expression showed a trend to be increased in RL vs. NAWM (p = 0.076, Fig. 4C), and FGFR1-3 expression did not significantly change between NAWM, AL, RL and IdL.

Oligodendrocyte differentiation has been shown to be influenced by the notch signaling pathway (Popko, 2003), which can either inhibit (Genoud et al., 2002; Wang et al., 1998) or promote oligodendrocyte maturation (Aparicio et al., 2013; Grandbarbe et al., 2003; Hu et al., 2003), depending on the stimulus. Here, we found a trend towards a higher expression of JAG1 in IdL in comparison to NAWM (p = 0.076). In contrast, activation by F3/contactin (CNTN1) promotes OPC differentiation/maturation (Aparicio et al., 2013). However, no significant difference in CNTN1 or CNTN2 expression was detected in MS tissues. NOTCH1 expression itself showed a trend towards being reduced in RL (p = 0.06) in comparison to NAWM.

CXCL12/CXCR4 signaling has been demonstrated to be involved in oligodendrogliogenesis (Dziembowska et al., 2005; Zilkha-Falb et al., 2016). In comparison to NAWM, CXCL12 expression was significantly

**Table 4**
Differential expression of genes involved in oligodendrogenesis.

Differential gene expression of genes known to be involved in oligodendrogenesis. Differential gene expression was analysed between all four different tissue types (AL, RL, IdL and NAWM). Table shows relative fold changes in between the different tissue types of a selection of genes known to be involved in oligodendrogenesis. Genes with a p-value of $< 0.05$ are shown in bold, and were colored according to their fold change. Genes with a fold change higher than 1.5 were marked red. Genes with a fold change lower than $-1.5$ were marked green.

| Symbol | Gene name | Relative fold changes | | | | | |
|---|---|---|---|---|---|---|---|
| | | AL vs. NAWM | RL vs. NAWM | IDL vs. NAWM | RL vs. AL | IDL vs. AL | RL vs. IDL |
| | ***Growth factors*** | | | | | | |
| BMP2 | bone morphogenetic protein 2 | 1.10 | 1.18 | 1.17 | 1.07 | 1.07 | 0.99 |
| FGF2 | fibroblast growth factor 2 | 1.52 | 1.20 | -1.08 | -1.26 | -1.64 | 1.30 |
| FGF9 | fibroblast growth factor 9 | 1.18 | 1.30 | 1.22 | 1.11 | 1.04 | 1.07 |
| IGF1 | insulin-like growth factor 1 | 1.71 | 1.69 | **3.33** | -1.01 | 1.95 | -1.97 |
| IGF2 | insulin-like growth factor 2 | 1.54 | -1.11 | **2.90** | -1.71 | 1.88 | **-3.21** |
| JAG1 | jagged 1 | 1.25 | 1.57 | 1.93 | 1.26 | 1.54 | -1.23 |
| NTF3 | neurotrophin 3 | 1.05 | -1.30 | -1.17 | -1.37 | -1.23 | -1.11 |
| PDGFA | plateled-derived growth factor, alpha polypeptide | -1.11 | 1.04 | 1.02 | 1.15 | 1.13 | 1.02 |
| | ***Receptors*** | | | | | | |
| CNTFR | ciliary neurotrophic factor receptor | 1.26 | 1.08 | 1.48 | -1.16 | 1.18 | -1.37 |
| EGFR | epidermal growth factor receptor | 1.29 | 1.31 | -1.03 | 1.01 | -1.33 | 1.34 |
| FGFR1 | fibroblast growth factor receptor 1 | 1.16 | 1.43 | 1.38 | 1.24 | 1.20 | 1.04 |
| FGFR2 | fibroblast growth factor receptor 2 | -1.10 | 1.27 | 1.12 | 1.40 | 1.23 | 1.14 |
| FGFR3 | fibroblast growth factor receptor 3 | -1.00 | 1.32 | 1.60 | 1.32 | 1.60 | -1.21 |
| FGFR4 | fibroblast growth factor receptor 4 | 1.36 | 2.16 | 1.68 | 1.59 | 1.24 | 1.29 |
| LIFR | leukemia inhibitory factor receptor alpha | -1.72 | -2.17 | -1.65 | -1.26 | 1.04 | -1.31 |
| NGFR | nerve growth factor receptor | -1.01 | 2.04 | 2.33 | 2.06 | 2.36 | -1.14 |
| NRP1 | neuropilin 1 | -1.04 | 1.12 | 1.05 | 1.17 | 1.09 | 1.07 |
| NRP2 | neuropilin 2 | -1.07 | 1.00 | 1.33 | 1.07 | 1.42 | -1.33 |
| SEMA4D | semaphorin 4D | 1.08 | 1.27 | 1.08 | 1.17 | -1.00 | 1.17 |
| P2RX7 | purinergic receptor P2X 7 | -1.43 | **-1.98** | **-2.13** | -1.38 | -1.49 | 1.08 |
| | ***Transcription factors*** | | | | | | |
| NOTCH1 | Notch1 | -1.06 | -1.38 | -1.07 | -1.30 | -1.01 | -1.29 |
| NKX2-2 | NK2 homeobox 2 | **-1.87** | -1.49 | **-2.37** | 1.25 | -1.27 | 1.59 |
| SOX2 | SRY-box 2 | 1.08 | 1.40 | 1.47 | 1.30 | 1.36 | -1.05 |
| SOX9 | SRY-box 9 | -1.03 | 1.08 | -1.10 | 1.11 | -1.07 | 1.19 |
| SOX10 | SRY-box 10 | -1.32 | -1.06 | **-2.70** | 1.25 | **-2.04** | **2.54** |

(*continued on next page*)

**Table 4** (*continued*)

| | | | | | | | |
|---|---|---|---|---|---|---|---|
| | ***Myelin genes*** | | | | | | |
| MAG | myelin-associated glycoprotein | -1.46 | -1.18 | **-3.37** | 1.24 | **-2.30** | **2.86** |
| MAL | myelin and lymphocyte protein | -1.42 | -1.59 | **-3.50** | -1.12 | **-2.47** | **2.20** |
| MBP | myelin basic protein | 1.31 | **1.81** | 1.68 | 1.38 | 1.28 | 1.07 |
| MOBP | myelin-associated oligodendrocytic basic protein | -1.43 | -1.71 | **-3.83** | -1.20 | **-2.68** | 2.24 |
| MOG | myelin oligodendrocyte glycoprotein | -1.44 | -1.46 | **-1.76** | -1.01 | -1.23 | 1.21 |
| PLP1 | proteolipid protein 1 | -1.52 | -2.01 | **-5.96** | -1.33 | **-3.93** | 2.96 |
| SCD | stearoyl-CoA desaturase | **-1.81** | **-2.54** | **-3.80** | -1.40 | **-2.10** | 1.50 |
| | ***Cytokines*** | | | | | | |
| CXCL12 | chemokine (C-X-C motif) ligand 12 | **1.88** | **2.25** | **2.76** | 1.20 | 1.47 | -1.22 |
| IL6 | interleukin 6 | 1.13 | -1.05 | -1.17 | -1.18 | -1.32 | 1.12 |
| LIF | leukemia inhibitory factor | -1.61 | -1.03 | -1.22 | 1.57 | 1.33 | 1.18 |
| | ***Others*** | | | | | | |
| CSPG4 | chondroitin sulfate proteoglycan 4 | -1.11 | 1.23 | 1.04 | 1.37 | 1.16 | 1.18 |
| TH | tyrosine hydroxylase | -1.11 | 1.24 | 1.24 | 1.38 | 1.37 | 1.01 |
| PTPN11 | protein tyrosine phosphatase, non-receptor type 11 | -1.09 | -1.46 | -1.68 | -1.34 | -1.54 | 1.15 |
| SEMA3B | semaphorin 3B | **-1.69** | **-1.66** | **-2.16** | 1.02 | -1.28 | 1.30 |
| RELN | reelin | 1.01 | -1.06 | -1.19 | -1.08 | -1.21 | 1.12 |
| NCAM1 | neural cell adhesion molecule 1 | -1.07 | -1.54 | **-2.14** | -1.44 | **-2.00** | 1.39 |
| VTN | vitronectin | -1.21 | -1.04 | -1.47 | 1.17 | -1.22 | 1.42 |
| TNC | tenascin C | 1.12 | 1.89 | **2.72** | 1.69 | **2.43** | -1.44 |
| THRB | thyroid hormone receptor, beta | -1.48 | 1.00 | -1.10 | 1.49 | 1.35 | 1.10 |
| MARCKS | myristoylated alanine rich protein kinase C substrate | 1.28 | -1.24 | **-2.11** | 1.58 | **-1.71** | **2.70** |
| GJB1 | gap junction protein beta 1 | -1.33 | -1.25 | **2.51** | -1.06 | **3.14** | **-3.34** |
| CNTN2 | contactin 2 | -1.20 | -1.60 | 1.51 | 1.34 | **2.24** | -1.81 |

higher in AL ($p = 0.019$), RL ($p = 0.006$) as well as IdL ($p = 0.002$) (Fig. 4C). In contrast, CXCR4 expression was not significantly changed between the different tissue types. Oligodendrocyte differentiation and maturation is further regulated by NKX2-2 (Qi et al., 2001). In the different tissue types, NKX2-2 expression was significantly lower in AL ($p = 0.008$) and IdL ($p = 0.003$), but not in RL (Fig. 4D). The terminal differentiation of oligodendrocytes is dependent on the transcription factor Sox10 (Stolt et al., 2002). The expression of SOX10 was significantly reduced in IdL in comparison to AL ($p = 0.032$), RL ($p = 0.007$) and NAWM ($p = 0.005$, Fig. 4E). Finally, SEMA3B has been shown to inhibit oligodendrocyte migration (Cohen et al., 2003). In our gene expression analysis, SEMA3B expression was significantly increased in NAWM in comparison to AL ($p = 0.019$), RL ($p = 0.041$) and IdL ($p = 0.006$, Fig. 4F).

### 3.5. Genes involved in the STAT6 signaling pathway are differentially expressed in lesion tissue

We have previously reported that members of the STAT6 signaling pathway are upregulated in NAWM in comparison to control WM (Zeis et al., 2008). Here we show that the expression of members of the STAT6 signaling pathway, such as STAT6 itself, IL4 and IL4R, is increased in AL, RL and IdL tissue (Table 5, Fig. 4G, H, I). STAT6 expression is significantly higher in AL, RL and IdL lesions (Fig. 4G). IL4 expression showed a strong tendency to be increased in RL in comparison to NAWM ($p = 0.051$) and in AL and IdL (Fig. 4H). Finally, IL4R expression was significantly higher in RL and IdL in comparison to NAWM. In AL, IL4R expression showed a trend towards being increased but not in all cases (Fig. 4I). Expression of JAK1 and JAK3 did not show any significant expression changes between NAWM, AL, RL and IdL.

### 3.6. Expression of myelin genes decreases from NAWM to IdL tissue

The expression of myelin genes MAG, MAL (Fig. 4J), MOBP, MOG (Fig. 4K), and PLP1 (Fig. 4L), with the exception of MBP, was not significantly changed in AL or RL in comparison to NAWM. In contrast, myelin gene expression was strongly reduced in IdL in comparison to NAWM (Table 4). However, MBP gene expression was significantly increased in RL in comparison to NAWM (Table 4).

### 3.7. Pathway analysis shows a strong immune activation in all tissues in comparison to NAWM

To investigate possible pathways and/or networks involved in

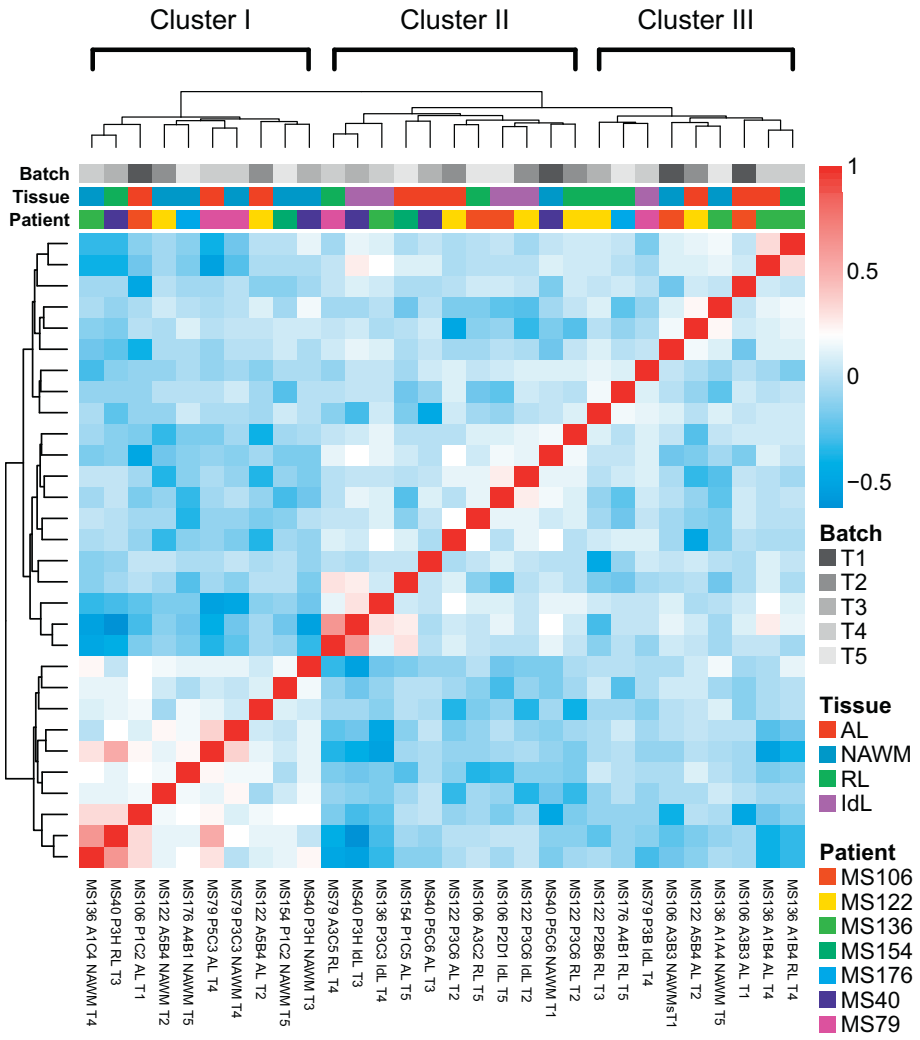


**Fig. 3.** Cluster analysis.
Cluster analysis of the gene expression data from all samples reveals three main clusters. Cluster 1 contained most of the NAWM tissue (6 out of 9) whereas in cluster 2 most IdL tissues were found. AL and RL tissues were dispersed in all three clusters. Clusters were not formed by possible confounding factors such as patient or batch.

lesion formation or resolution, we performed an Ingenuity pathway core analysis between all different tissue types (Table 6). Compared to NAWM, an increased *proliferation of immune cells* was predicted in all lesion types (activation z-score; AL: 1.806, RL: 2.296, IdL: 2.434). Moreover, an increased activation of many different immune system functions was predicted in AL, RL and IdL in comparison to NAWM (Table 6). Interestingly, a significant activation of *development of neurons* pathways was predicted in AL tissue in comparison to NAWM ($p = 2.08E-12$, activation z-score = 2.672). In addition, *cell viability of neuroglia* was also predicted to be increased in AL ($p = 3.89E-13$, activation z-score = 2.260). In the comparison of RL vs NAWM, an increase of *myelination* was predicted ($p = 3.28E-15$, activation z-score = 2.170).

Comparison between AL and RL revealed a predicted decrease in several functions associated with immune system function such as, *cell movement of phagocytes* ($p = 6.26E-27$, activation z-score = −3.419) and *leukocyte migration* ($p = 1.07E-31$, activation z-score = −2.768) in the AL tissue. Finally, analysis of the differential gene expression between RL and IdL revealed a predicted increase of *lymphocyte stimulation* ($p = 1.18E-09$, activation z-score = 2.211) and genes involved in *systemic autoimmune disease* ($p = 7.03E-19$, activation z-score = 2.672).

### 3.8. qRT-PCR verification

To verify the results of the differential gene expression study, we performed a qRT-PCR analysis on a different set of tissues from 9 different MS patients. In total the expression of IGF2, CXCL12, STAT6, NPY, MAG as well as MAL was analysed on 22 NAWM, 14 AL, 8 RL and 9 IdL tissue samples (Table 7). Overall, qRT-PCR confirmed the results from the ATLAS cDNA gene expression array. In the comparison of RL vs NAWM, NPY, STAT6 and MAG showed a similar increase or decrease in expression in qRT-PCR as in the array study, but without significance (NPY; $p = 0.105$, STAT6; $p = 0.300$, MAG; $p = 0.149$).

## 4. Discussion

We have previously shown that there is a balance between proinflammatory genes, expressed mainly by microglia, and anti-inflammatory and neuroprotective genes, expressed predominantly by oligodendrocytes in the MS NAWM in comparison to control (Graumann et al., 2003; Zeis et al., 2008; Zeis et al., 2009). Therefore, it might be expected that a shift in the balance of these opposing processes might lead to the formation of lesions. To investigate this further, we analysed the gene expression of normal appearing white matter (NAWM), active, remyelinating and inactive demyelinating lesions with

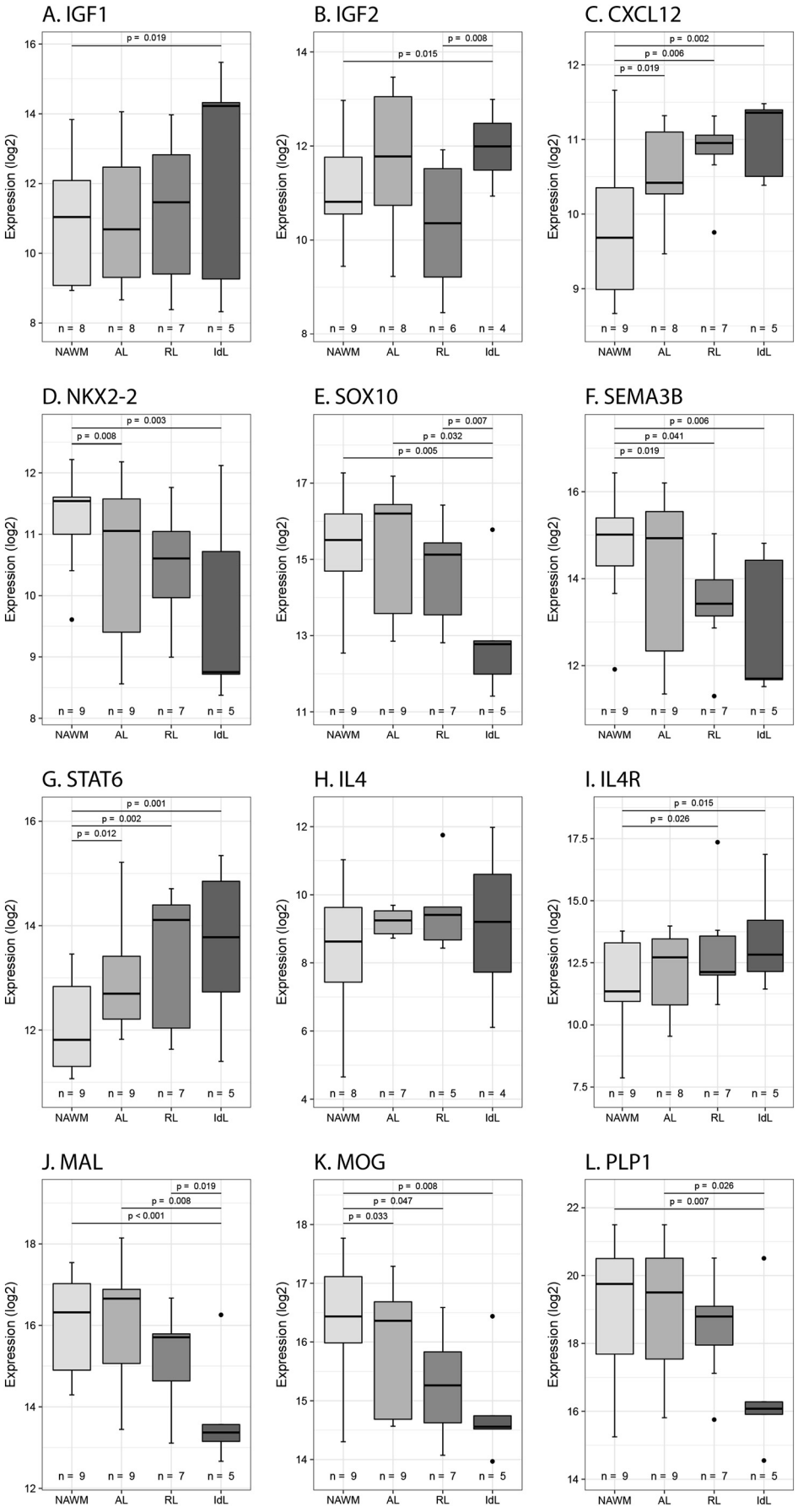


**Fig. 4.** Boxplots of selected genes.
Boxplots of differential gene expression between NAWM, AL, RL and IdL of selected genes are shown. A high variability in between samples of the same tissue type is visible for different genes, such as e.g. IGF1 (A), NKX2-2 (D, AL & IdL) and SEMA3B (F, AL). Whereas IGF1 (A) and IGF2 (B) expression shows no clear trend between the different tissue types, the expression of CXCL12 (C) is increased from NAWM to IdL lesion tissues. In contrast, the expression of NKX2-2 (D), SOX10 (E) and SEMA3B (F) are decreased from NAWM to IdL tissue. The expression of STAT6 (G) and IL4 (H) tend to be the highest in RL tissue, whereas the expression of IL4R (I) is highest in IdL. As expected, the expression of the myelin genes MAL (J), MOG (K) and PLP1 (M) is lowest in IdL tissues.

**Table 5**
Differential expression of STAT6 pathway genes.

Differential gene expression of genes of the STAT6 pathway. Relative fold changes are shown. Differential expression was analysed between AL, RL and IdL in comparison to NAWM. Statistically significant changes are marked in bold red.

| | Gene | NAWM | AL | RL | IdL |
|---|---|---|---|---|---|
| STAT6 Pathway | STAT6 | 1 | **1.99** | **2.7** | **3.1** |
| | JAK1 | 1 | 1.1 | 0.83 | 1.12 |
| | JAK3 | 1 | 0.67 | 0.76 | 0.88 |
| | IL4 | 1 | 2.07 | **3.47** | 1.99 |
| | IL4R | 1 | 2.35 | **4.43** | **5.9** |

a focus on genes known to be involved in oligodendrocyte development and regeneration. By comparing the gene expression of the different tissue types, representative for lesion developmental stages, we speculated that depending on the comparison made, genes involved in various processes influencing lesion growth, repair or inactivation might be detected. We expected that genes involved in lesion growth and/or inflammatory processes might be detected in NAWM vs AL, whereas genes playing a role in lesion clearance/repair would be detected in the AL vs RL comparison. Comparing RL vs IdL might have been expected to reveal genes that play a role in either blocking or initiating/promoting remyelination. Our results show that our hypothesis was partially validated (Table 6). However, heterogeneity of gene expression in individual categories and, in retrospect the use of too broad a lesion staging process, made it challenging to detect clear differences between the data sets.

**Table 6**
Ingenuity pathway analysis.

Ingenuity pathway analysis of the differential gene expression between NAWM, AL, RL and IdL. Differential gene expression between NAWM, AL, RL and IdL was analysed to predict the increase/decrease of activation of particular functions in the different tissues. A selection of functions predicted to be activated/inhibited is shown.

| Biological function annotation | p-Value | Predicted activation | Activation z-score |
|---|---|---|---|
| AL vs NAWM | | | |
| Development of neurons | 2.08E-12 | Increased | 2.672 |
| Cell viability of central nervous system cells | 6.95E-12 | Increased | 2.478 |
| Cell viability of neuroglia | 3.89E-13 | Increased | 2.26 |
| Cell viability of myeloid cells | 2.79E-13 | Increased | 2.138 |
| Stimulation of myeloid cells | 1.31E-12 | Increased | 2.046 |
| Axonogenesis | 2.33E-11 | Increased | 2.019 |
| RL vs NAWM | | | |
| Leukocyte migration | 8.34E-37 | Increased | 2.651 |
| Development of neurons | 3.23E-14 | Increased | 2.616 |
| Cell proliferation of T lymphocytes | 4.49E-21 | Increased | 2.456 |
| Proliferation of immune cells | 1.71E-22 | Increased | 2.296 |
| Proliferation of neuronal cells | 4.42E-15 | Increased | 2.257 |
| Myelination | 3.28E-15 | Increased | 2.17 |
| IdL vs NAWM | | | |
| Proliferation of lymphocytes | 2.86E-34 | Increased | 2.728 |
| Proliferation of mononuclear leukocytes | 4.67E-36 | Increased | 2.672 |
| Proliferation of immune cells | 1.87E-37 | Increased | 2.434 |
| T cell migration | 1.15E-19 | Increased | 2.14 |
| AL vs RL | | | |
| Cell movement of phagocytes | 6.26E-27 | Decreased | −3.419 |
| Leukocyte migration | 1.07E-31 | Decreased | −2.768 |
| Cellular infiltration by macrophages | 2.38E-13 | Decreased | −2.692 |
| T cell response | 3.40E-10 | Decreased | −2.33 |
| Proliferation of immune cells | 3.10E-18 | Decreased | −2.294 |
| AL vs IdL | | | |
| Inflammation of organ | 1.29E-39 | Increased | 2.748 |
| Viral Infection | 9.85E-26 | Increased | 2.308 |
| Cell proliferation of tumor cell lines | 1.96E-28 | Increased | 2.19 |
| RL vs IdL | | | |
| Systemic autoimmune syndrome | 7.03E-19 | Increased | 2.672 |
| Inflammation of organ | 1.17E-23 | Increased | 2.522 |
| Stimulation of T lymphocytes | 1.74E-08 | Increased | 2.319 |
| Stimulation of lymphocytes | 1.18E-09 | Increased | 2.211 |
| Chemotaxis of granulocytes | 5.04E-09 | Increased | 2.154 |

**Table 7**
qRT-PCR verification.

To verify the results from the ATLAS cDNA gene expression array we performed a quantitative RT-PCR analysis of selected genes. In a majority of comparisons the results from the ATLAS cDNA expression array matched with the qRT-PCR analysis.

| Gene | AL vs NAWM | | RM vs NAWM | | IdL vs NAWM | |
|---|---|---|---|---|---|---|
| | Array | qPCR | Array | qPCR | Array | qPCR |
| MAL | −1.42 | −1.93 | −1.59 | −1.80 | −3.50 | −3.85 |
| MAG | −1.46 | −1.47 | −1.18 | −1.38 | −3.37 | −2.83 |
| IL4R | 2.35 | 1.31 | 4.43 | 1.18 | 5.9 | 1.43 |
| STAT6 | 1.99 | 1.58 | 2.7 | 1.16 | 3.1 | 1.71 |
| CXCL12 | 1.88 | 1.92 | 2.25 | 2.02 | 2.76 | 3.56 |
| IGF2 | 1.54 | 1.22 | −1.11 | 1.25 | 2.90 | 2.22 |

The expression of many genes varied strongly across the different types of white matter tissue seen in the MS brain (NAWM, AL, RL, IdL). For example, the expression of the IGF1 gene varied by > 128 fold between the different IdL tissue samples (Fig. 4A), even though these tissue samples were similar at the immunohistochemical level. This heterogeneity could result from the different stages of lesion development and resolution in the samples, which would lead to changes in cell populations, or different pathogenetic mechanisms. Such variability in the expression of genes influencing oligodendrocyte development might be one of the causes for heterogeneous lesion outcome in MS patients. Lesion specific signaling, originating from the interplay between the different cells present, might lead to the reported phenomenon that in a single patient both successful remyelination and remyelination failure is detected (Patrikios et al., 2006).

There are potentially many causes for remyelination failure; non-disease-related factors age, sex, genetic background; (Franklin and Ffrench-Constant, 2008), insufficient OPC availability (Ludwin, 1980; Mason et al., 2004), insufficient OPC migration (Boyd et al., 2013), deficient OPC differentiation, proliferation or myelination (Franklin and Ffrench-Constant, 2008; Wolswijk, 1998) or compromised axons unable to support their remyelination (Chang et al., 2002). Our results show that even in inactive demyelinated lesions, factors are present that could initiate and/or support remyelination (e.g. IGF1, IGF2 or CXCL12). We speculate that, although such factors are present, the simultaneous presence of factors opposing oligodendrocyte development (e.g. JAG1 (Wang et al., 1998)) might shift the balance in favor of demyelination. We also found an elevated expression of genes known to inhibit oligodendrogliogenesis in remyelinating lesion tissue (e.g. EDN1, TNC). We suggest that in this case, the expression of factors promoting remyelination exerted a stronger effect and neutralized the effects of genes inhibiting oligodendrocyte development, leading to successful remyelination. Furthermore, the timing of expression of developmental factors is crucial in oligodendrocyte development (Franklin, 2002; Franklin and Ffrench-Constant, 2008). Many factors can promote specific steps in oligodendrocyte development but have inhibiting properties at other stages. This is true for FGF2 or PDGF, which both promote OPC proliferation. Later however, PDGF slows down and FGF2 even inhibits differentiation (McKinnon et al., 1993).

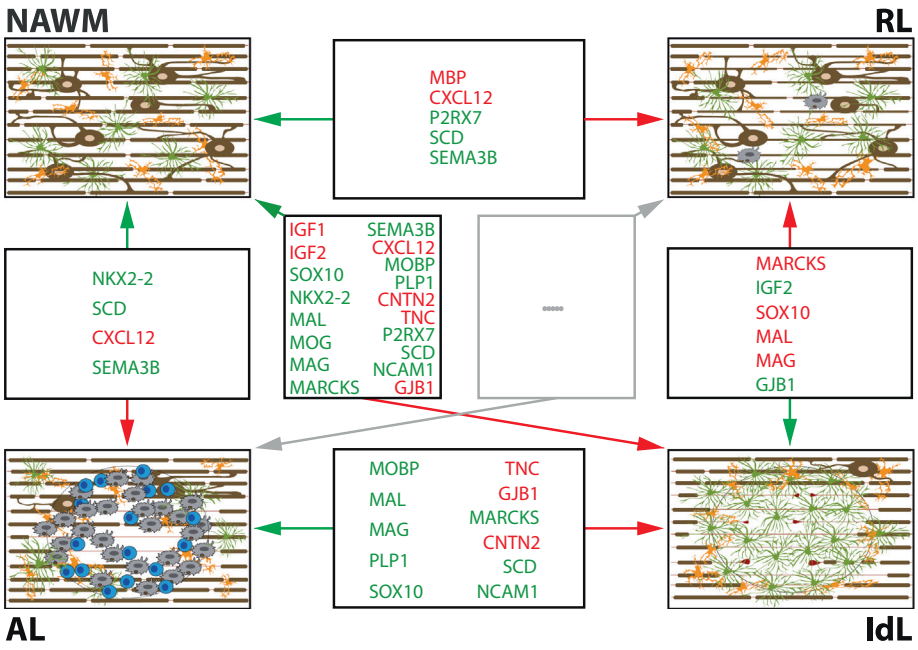


**Fig. 5.** Schematic drawing summarising the differential expression pattern of genes involved in oligodendrogliogenesis.
Summary scheme showing significantly differentially expressed genes involved in oligodendrogliogenesis between the different tissue types (Table 4). Genes are color coded according to their higher (green) or lower (red) expression in the tissue the color matching arrow points to. (For interpretation of the references to color in this figure legend, the reader is referred to the web version of this article.)

Therefore, genes normally beneficial in oligodendrocyte development might be detrimental for remyelination if expressed at the wrong time point. Altogether, we did not detect a clear pro- or anti- oligodendrogliogenesis/remyelinating gene expression pattern in the different types of lesions (Fig. 5).

We previously reported an increased expression of STAT6 in the NAWM of MS patients in comparison to control patients (Zeis et al., 2008; Zeis et al., 2009). Furthermore, we demonstrated that in the NAWM, STAT6 is expressed mainly by oligodendrocytes and to a minor extent in astrocytes (Zeis et al., 2008). Interestingly, we found that STAT6, as well as two members of the STAT6 pathway, IL4 and IL4R, are higher expressed in AL, RL and IdL in comparison to NAWM. This suggests that a possible protective, anti-inflammatory reaction already activated in the NAWM, is intensified in zones of ongoing inflammation in MS, although other non-immunological related functions cannot be ruled out (Zeis et al., 2016).

Pathway analysis of the differential gene expression between the different tissues is particularly difficult due to the highly variable cellular composition (Fig. 1). This might result in a different RNA pool and, therefore, the resulting differential gene expression is predominantly defined by the change in cell type composition and changes in gene expression of resident cells might be masked. This is reflected by the results of the biological function analysis, which showed that the most enriched processes detected were related to the immune system (Table 6). However, in addition to that, we found a signature of an increased *development of neurons*, *cell viability of CNS cells* and *axonogenesis* in AL and *myelination* in RL tissue when compared with NAWM tissue. These signatures suggest that glial cells react to the inflammation with a protective response and/or infiltrating immune cells support the survival of resident cells by expressing genes supportive of cell viability.

Understanding the signaling pathways leading to lesion remyelination in MS is key for devising therapies that enhance repair. Our study was designed to identify common factors that might distinguish the different tissue types (NAWM, AL, RL and IdL) and serve as therapeutic candidates to enhance remyelination. In summary, several different factors known to be involved in oligodendrocyte development were detected to be differentially regulated between the different tissue types (summarized in Fig. 5). However, no specific de- or remyelinating pattern was detected in either tissue type; rather a largely heterogeneous expression pattern of oligodendrogliogenesis influencing genes was detected between, but also within, the different lesion types. This indicates that at any one point in time in the MS brain, developing and repairing lesions can be present at many different stages, in keeping with a continuum of ongoing processes. A greater understanding of this heterogeneity is crucial if we are to understand the correct timing for delivery of agents that enhance remyelination. Therefore, a precise characterization of the temporal and spatial localization of pro-repair factors is required.

Supplementary data to this article can be found online at https://doi.org/10.1016/j.expneurol.2018.03.012.

## Author contribution

N.·S-W. contributed to study design, oversight and manuscript preparation. R.R. contributed to study design, oversight and sample selection. O.H. contributed to sample selection and characterization, RNA isolation and array hybridization. T.Z. performed the data analysis and interpretation, qPCR and manuscript preparation.

## Acknowledgements

The authors would like to thank Florian Geier and Robert Ivanek of the Bioinformatics Core Facility of the Department of Biomedicine for support with the statistical analysis. We thank Christine Stadelmann for critically reading the manuscript and helpful discussions. The authors would like to thank the UK MS Tissue Bank at Imperial College for the provision of tissue for this study. This study was supported by the UK MS Society (Grant 619/01 to NSW and RR), National Multiple Sclerosis Society of the United States of America (Grant RG 3583A1 and RG 4249A2 to NSW), by the Swiss Multiple Sclerosis Society, the French MS Society (ARSEP), and by the Swiss National Science Foundation (31003A_159528/1) all to NSW. The authors declare no conflict of interest.

## References

Aparicio, E., Mathieu, P., Pereira Luppi, M., Almeira Gubiani, M.F., Adamo, A.M., 2013. The Notch signaling pathway: its role in focal CNS demyelination and apotransferrin-induced remyelination. J. Neurochem. 127, 819–836.
Barnett, M.H., Prineas, J.W., 2004. Relapsing and remitting multiple sclerosis: pathology of the newly forming lesion. Ann. Neurol. 55, 458–468.
Beck, K.D., Powell-Braxton, L., Widmer, H.R., Valverde, J., Hefti, F., 1995. Igf1 gene

disruption results in reduced brain size, CNS hypomyelination, and loss of hippocampal granule and striatal parvalbumin-containing neurons. Neuron 14, 717–730.
Boyd, A., Zhang, H., Williams, A., 2013. Insufficient OPC migration into demyelinated lesions is a cause of poor remyelination in MS and mouse models. Acta Neuropathol. 125, 841–859.
Carson, M.J., Behringer, R.R., Brinster, R.L., McMorris, F.A., 1993. Insulin-like growth factor I increases brain growth and central nervous system myelination in transgenic mice. Neuron 10, 729–740.
Chang, A., Tourtellotte, W.W., Rudick, R., Trapp, B.D., 2002. Premyelinating oligodendrocytes in chronic lesions of multiple sclerosis. N. Engl. J. Med. 346, 165–173.
Cohen, R.I., Rottkamp, D.M., Maric, D., Barker, J.L., Hudson, L.D., 2003. A role for semaphorins and neuropilins in oligodendrocyte guidance. J. Neurochem. 85, 1262–1278.
Compston, A., Coles, A., 2002. Multiple sclerosis. Lancet 359, 1221–1231.
Compston, A., McDonald, I., Noseworthy, J., Lassmann, H., Miller, D., Smith, K., Wekerle, H., Confavreux, C., 2006. McAlpine's Multiple Sclerosis. Churchill Livingstone.
Dziembowska, M., Tham, T.N., Lau, P., Vitry, S., Lazarini, F., Dubois-Dalcq, M., 2005. A role for CXCR4 signaling in survival and migration of neural and oligodendrocyte precursors. Glia 50, 258–269.
Erne, B., Sansano, S., Frank, M., Schaeren-Wiemers, N., 2002. Rafts in adult peripheral nerve myelin contain major structural myelin proteins and myelin and lymphocyte protein (MAL) and CD59 as specific markers. J. Neurochem. 82, 550–562.
Filippi, M., Rocca, M.A., Martino, G., Horsfield, M.A., Comi, G., 1998. Magnetization transfer changes in the normal appearing white matter precede the appearance of enhancing lesions in patients with multiple sclerosis. Ann. Neurol. 43, 809–814.
Fortin, D., Rom, E., Sun, H., Yayon, A., Bansal, R., 2005. Distinct fibroblast growth factor (FGF)/FGF receptor signaling pairs initiate diverse cellular responses in the oligodendrocyte lineage. J. Neurosci. 25, 7470–7479.
Franklin, R.J., 2002. Why does remyelination fail in multiple sclerosis? Nat. Rev. Neurosci. 3, 705–714.
Franklin, R.J., Ffrench-Constant, C., 2008. Remyelination in the CNS: from biology to therapy. Nat. Rev. Neurosci. 9, 839–855.
Furusho, M., Dupree, J.L., Nave, K.A., Bansal, R., 2012. Fibroblast growth factor receptor signaling in oligodendrocytes regulates myelin sheath thickness. J. Neurosci. 32, 6631–6641.
Gautier, H.O., Evans, K.A., Volbracht, K., James, R., Sitnikov, S., Lundgaard, I., James, F., Lao-Peregrin, C., Reynolds, R., Franklin, R.J., Karadottir, R.T., 2015. Neuronal activity regulates remyelination via glutamate signalling to oligodendrocyte progenitors. Nat. Commun. 6, 8518.
Genoud, S., Lappe-Siefke, C., Goebbels, S., Radtke, F., Aguet, M., Scherer, S.S., Suter, U., Nave, K.A., Mantei, N., 2002. Notch1 control of oligodendrocyte differentiation in the spinal cord. J. Cell Biol. 158, 709–718.
Grandbarbe, L., Bouissac, J., Rand, M., Hrabe de Angelis, M., Artavanis-Tsakonas, S., Mohier, E., 2003. Delta-Notch signaling controls the generation of neurons/glia from neural stem cells in a stepwise process. Development 130, 1391–1402.
Graumann, U., Reynolds, R., Steck, A.J., Schaeren-Wiemers, N., 2003. Molecular changes in normal appearing white matter in multiple sclerosis are characteristic of neuroprotective mechanisms against hypoxic insult. Brain Pathol. 13, 554–573.
Hemmer, B., Archelos, J.J., Hartung, H.P., 2002. New concepts in the immunopathogenesis of multiple sclerosis. Nat. Rev. Neurosci. 3, 291–301.
Hu, Q.D., Ang, B.T., Karsak, M., Hu, W.P., Cui, X.Y., Duka, T., Takeda, Y., Chia, W., Sankar, N., Ng, Y.K., Ling, E.A., Maciag, T., Small, D., Trifonova, R., Kopan, R., Okano, H., Nakafuku, M., Chiba, S., Hirai, H., Aster, J.C., Schachner, M., Pallen, C.J., Watanabe, K., Xiao, Z.C., 2003. F3/contactin acts as a functional ligand for Notch during oligodendrocyte maturation. Cell 115, 163–175.
Huang, Y., Dreyfus, C.F., 2016. The role of growth factors as a therapeutic approach to demyelinating disease. Exp. Neurol. 283, 531–540.
Kuhlmann, T., Ludwin, S., Prat, A., Antel, J., Bruck, W., Lassmann, H., 2017. An updated histological classification system for multiple sclerosis lesions. Acta Neuropathol. 133, 13–24.
Lassmann, H., 1998. Neuropathology in multiple sclerosis: new concepts. Mult. Scler. 4, 93–98.
Lindberg, R.L., De Groot, C.J., Certa, U., Ravid, R., Hoffmann, F., Kappos, L., Leppert, D., 2004. Multiple sclerosis as a generalized CNS disease—comparative microarray analysis of normal appearing white matter and lesions in secondary progressive MS. J. Neuroimmunol. 152, 154–167.
Lindner, M., Thummler, K., Arthur, A., Brunner, S., Elliott, C., McElroy, D., Mohan, H., Williams, A., Edgar, J.M., Schuh, C., Stadelmann, C., Barnett, S.C., Lassmann, H., Mucklisch, S., Mudaliar, M., Schaeren-Wiemers, N., Meinl, E., Linington, C., 2015. Fibroblast growth factor signalling in multiple sclerosis: inhibition of myelination and induction of pro-inflammatory environment by FGF9. Brain 138, 1875–1893.
Ludwin, S.K., 1980. Chronic demyelination inhibits remyelination in the central nervous system. An analysis of contributing factors. Lab. Investig. 43, 382–387.
Mason, J.L., Toews, A., Hostettler, J.D., Morell, P., Suzuki, K., Goldman, J.E., Matsushima, G.K., 2004. Oligodendrocytes and progenitors become progressively depleted within chronically demyelinated lesions. Am. J. Pathol. 164, 1673–1682.
McKinnon, R.D., Matsui, T., Dubois-Dalcq, M., Aaronson, S.A., 1990. FGF modulates the PDGF-driven pathway of oligodendrocyte development. Neuron 5, 603–614.
McKinnon, R.D., Smith, C., Behar, T., Smith, T., Dubois-Dalcq, M., 1993. Distinct effects of bFGF and PDGF on oligodendrocyte progenitor cells. Glia 7, 245–254.
McMorris, F.A., Smith, T.M., DeSalvo, S., Furlanetto, R.W., 1986. Insulin-like growth factor I/somatomedin C: a potent inducer of oligodendrocyte development. Proc. Natl. Acad. Sci. U. S. A. 83, 822–826.
Noseworthy, J.H., Lucchinetti, C., Rodriguez, M., Weinshenker, B.G., 2000. Multiple sclerosis. N. Engl. J. Med. 343, 938–952.
Patrikios, P., Stadelmann, C., Kutzelnigg, A., Rauschka, H., Schmidbauer, M., Laursen, H., Sorensen, P.S., Bruck, W., Lucchinetti, C., Lassmann, H., 2006. Remyelination is extensive in a subset of multiple sclerosis patients. Brain 129, 3165–3172.
Phipson, B., Lee, S., Majewski, I.J., Alexander, W.S., Smyth, G.K., 2016. Robust Hyperparameter estimation protects against Hypervariable genes and improves power to detect differential expression. Ann. Appl. Stat. 10, 946–963.
Popko, B., 2003. Notch signaling: a rheostat regulating oligodendrocyte differentiation? Dev. Cell 5, 668–669.
Prineas, J.W., Kwon, E.E., Goldenberg, P.Z., Ilyas, A.A., Quarles, R.H., Benjamins, J.A., Sprinkle, T.J., 1989. Multiple sclerosis. Oligodendrocyte proliferation and differentiation in fresh lesions. Lab. Investig. 61, 489–503.
Qi, Y., Cai, J., Wu, Y., Wu, R., Lee, J., Fu, H., Rao, M., Sussel, L., Rubenstein, J., Qiu, M., 2001. Control of oligodendrocyte differentiation by the Nkx2.2 homeodomain transcription factor. Development 128, 2723–2733.
R developmental Core Team, 2008. R: A Language and Environment for Statistical Computing.
Raine, C.S., Wu, E., 1993. Multiple sclerosis: remyelination in acute lesions. J. Neuropathol. Exp. Neurol. 52, 199–204.
Ritchie, M.E., Phipson, B., Wu, D., Hu, Y., Law, C.W., Shi, W., Smyth, G.K., 2015. Limma powers differential expression analyses for RNA-sequencing and microarray studies. Nucleic Acids Res. 43, e47.
Stolt, C.C., Rehberg, S., Ader, M., Lommes, P., Riethmacher, D., Schachner, M., Bartsch, U., Wegner, M., 2002. Terminal differentiation of myelin-forming oligodendrocytes depends on the transcription factor Sox10. Genes Dev. 16, 165–170.
Trapp, B.D., 2004. Pathogenesis of multiple sclerosis: the eyes only see what the mind is prepared to comprehend. Ann. Neurol. 55, 455–457.
van der Valk, P., Amor, S., 2009. Preactive lesions in multiple sclerosis. Curr. Opin. Neurol. 22, 207–213.
Wang, S., Sdrulla, A.D., diSibio, G., Bush, G., Nofziger, D., Hicks, C., Weinmaster, G., Barres, B.A., 1998. Notch receptor activation inhibits oligodendrocyte differentiation. Neuron 21, 63–75.
Wolswijk, G., 1998. Chronic stage multiple sclerosis lesions contain a relatively quiescent population of oligodendrocyte precursor cells. J. Neurosci. 18, 601–609.
Zeis, T., Graumann, U., Reynolds, R., Schaeren-Wiemers, N., 2008. Normal-appearing white matter in multiple sclerosis is in a subtle balance between inflammation and neuroprotection. Brain 131, 288–303.
Zeis, T., Probst, A., Steck, A.J., Stadelmann, C., Bruck, W., Schaeren-Wiemers, N., 2009. Molecular changes in white matter adjacent to an active demyelinating lesion in early multiple sclerosis. Brain Pathol. 19, 459–466.
Zeis, T., Enz, L., Schaeren-Wiemers, N., 2016. The immunomodulatory oligodendrocyte. Brain Res. 1641, 139–148.
Zilkha-Falb, R., Kaushansky, N., Kawakami, N., Ben-Nun, A., 2016. Post-CNS-inflammation expression of CXCL12 promotes the endogenous myelin/neuronal repair capacity following spontaneous recovery from multiple sclerosis-like disease. J. Neuroinflammation 13, 7.
Zoupi, L., Savvaki, M., Kalemaki, K., Kalafatakis, I., Sidiropoulou, K., Karagogeos, D., 2018. The function of contactin-2/TAG-1 in oligodendrocytes in health and demyelinating pathology. Glia 66, 576–591.